Optothermomechanical Device for the Interferometric Characterization of Fibers

A. A. Hamza, T. Z. N. Sokkar, K. A. El-Farahaty, H. M. El-Dessouky

Physics Department, Faculty of Science, Mansoura University, Mansoura 35516, Egypt

Received 5 February 2004; accepted 8 June 2004
DOI 10.1002/app.21118
Published online in Wiley InterScience (www.interscience.wiley.com).

ABSTRACT: An optothermomechanical (OTM) device was designed and constructed for fiber characterization with a double-beam interference microscope. This device enabled us to correlate both the mechanical properties and the thermal properties with the optical properties of fibers. The OTM device consisted of three parts, which were used for the drawing (stress–strain), cooling, and heating of the fibers. The designed OTM device (cooling and heating) was attached to the Pluta microscope for the determination of the optical properties of high-density polyethylene (PE) fibers at different temperatures (0–50°C). Also, this OTM device (drawing and heating), connected to the Pluta microscope, was used to study the influence of the temperature (10–50°C) and draw ratio (1–7) simultaneously on the optical properties of polypropylene (PP) fibers. Microinterferograms were provided for illustration. © 2004 Wiley Periodicals, Inc. J Appl Polym Sci 95: 647–658, 2005

Key words: fibers; polyethylene (PE); poly(propylene) (PP); strain; stress

INTRODUCTION

Temperature is one of the important factors controlling stress–strain (σ–ε) curves. The irreversible deformation of polymers is associated with a considerable amount of dissipated energy (ca. 10–10^3 J). When the deformation rate is high enough, a considerable fraction of this energy can be absorbed by the sample and cause self-heating of the material.[1] A major feature of the behavior of amorphous or partially crystalline polymeric materials is the glass transition. At low temperatures, most plastics become hard and brittle, whereas at high temperatures, they are rubbery or leathery and have great flexibility and toughness. The glass-transition temperature (T_g) is attributed to a major change in the segmental mobility of the polymer chains. Above T_g, there is sufficient mobility, whereas below it, the chains are frozen in their positions.[2]

Temperature is an important operator that controls the stretching process of synthetic fibers. During stretching, there is a balance between two parameters: the temperature and strain rate. A low stretching temperature implies little chain relaxation, but in this case, the strain rate takes low values, leading, on the contrary, to larger chain relaxation.[3]

Drawing (σ–ε) is an important operation that improves the textile characteristics of manmade fibers. Undrawn synthetic fibers are almost isotropic in their physical properties. They exhibit low tenacity, low modulus of elasticity, high plastic deformability, and so forth. To turn them into useful fibers for textile and industrial use requires mechanical drawing. This results in stronger, more birefringent fibers that are highly anisotropic. Besides various techniques (e.g., infrared, ultraviolet, nuclear magnetic resonance, and X-ray spectroscopy), microinterferometric measurement [refractive indices and birefringence (Δn)] is a valuable tool for the characterization of these fibers. For instance, Δn of undrawn and drawn fibers is a useful parameter for the adjustment of the drawing process.[4] To optimize any technical drawing process, one should know the relationships between the undrawn material structure and the structural properties of the drawn fibers. One of these useful relationships is the σ–ε curve of undrawn fibers, which provides the yield stress (σ_y), the tensile modulus, and the stability of deformation for these fibers.[1]

Drawing (stretching) is one of the most common methods for changing the structure of a polymeric material to strengthen it during processing. This orients its chains and supermolecular structures. If the polymer is an amorphous one with molecules of regular structures, it may even crystallize.[2] The degree of axial orientation, often characterized by optical birefringence, increases with increasing draw ratio (D). The degree of orientation effectively produced in the drawing process depends on D, the drawing conditions, and the composition of the fiber.[1]

Drawing a fiber at room temperature is known as cold drawing and concerns the deformation of the pre-existing structure of the fiber. In the drawing–

Correspondence to: A. A. Hamza (hamzaaa@mans.edu.eg).

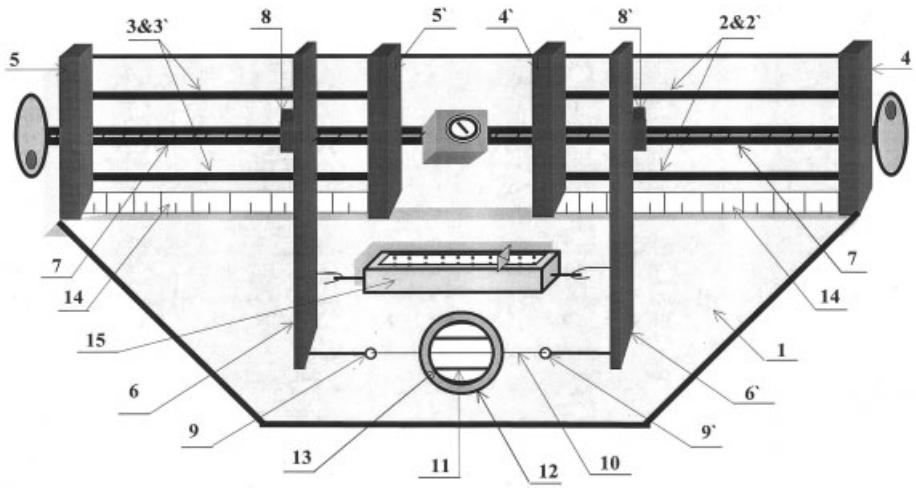

Figure 1 Schematic diagram of the OTM device and the drawing (σ–ε) setup.

stretching process, the changes in the optical properties can be determined by interferometric methods. Thus, the influence of D upon the structural changes occurring in the synthetic fibers is also indicated. Molecules are oriented parallel to the fiber axis, and drawing may produce a fringed fibril structure with the molecules lying parallel to the axis of the crystalline fiber.[5] The initial effect of the stretching will be increased alignment of the fibrils, thus increasing the transverse orientation of the molecules. If the stretching is continued, this will be followed by a change to the longitudinal orientation of the molecules.[6]

A double-beam interference (Pluta) microscope[7,8] is used to measure the refractive indices ($n^{\parallel}$ and $n^{\perp}$) of fibers for plane-polarized light vibrating parallel and perpendicularly to the fiber axis and Δn. These optical parameters characterize the structures of fibers, play an important role in the elucidation of the molecular arrangement within these fibers, and provide useful information about the processability of the fibers. The study of the aforementioned optical properties of fibers at different temperatures throws light on the optothermal behavior of the investigated fibers. Hamza and coworkers[9–13] made several attempts to study the influence of temperature or drawing on the optical and structural properties of fibers.

The samples discussed in this article are polyethylene (PE) fibers with a wide variety of grades and low-, medium-, and high-density formulations. The low-density types are flexible and tough. The medium-density and high-density types are stronger, harder, and more rigid. All are lightweight, easy-to-process, low-cost materials that have poor dimensional stability and heat resistance but excellent chemical resistance and electrical properties. Polypropylene (PP) fibers are also used because of their versatility, low density, excellent chemical resistance to acids and alkalis, easy processing, and low cost in comparison with other synthetic fibers. The impact toughness and other mechanical properties of its blends with other polymers are influenced by its crystallization and morphology, in addition to the physical and mechanical properties of each component, the state of dispersion, the interfacial adhesion, and so forth.[14,15]

We have designed an optothermomechanical (OTM) device to study the optothermal and optomechanical properties of fibers. We have studied the optothermal behavior of high-density polyethylene (HDPE) fibers with the cooling (under room temperature) and heating (above room temperature) parts of the OTM device at 0–50°C. We have also studied the OTM behavior of PP fibers with the drawing and heating parts of the OTM device. This setup is considered to be major improvement of this method for characterizing fibers during drawing. In this article, the σ–ε curve is examined to determine some mechanical parameters for PP fibers. The relationship between the refractive index and both D and the temperature for PP fibers is investigated. Two different types of polarization [the induced polarizability (p_i) and the permanent dipole moment (ξ_0)] of PP fibers are studied at different D values. The relationship between Δn and the average work per chain (W') is also examined.

DESIGN AND CHARACTERIZATION OF OTM DEVICE

Part i: Schematic diagram of the OTM device and drawing setup

This part is shown in Figure 1, in which the principal base (1) of the device (44 cm long, 26 cm wide, and 0.15 cm thick) is made from stainless steel. A stretching group consists of four sliding rods (2, 2′, 3, and 3′), which are supported with the principal base by four fixed bars (4, 4′, 5, and 5′). These bars are used for

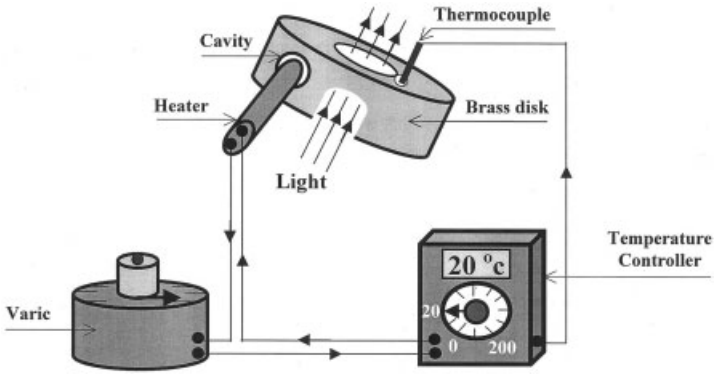

Figure 2 Schematic diagram of the heating setup.

guiding the motion of two movable bars (6 and 6′). Each bar moves on two sliding rods to ensure satisfactorily smooth and parallel movement.

The device is provided with a special rod (7), which is fixed to the center of the base (1). This rod is threaded as two halves. The first half is working as a left-handed thread, and the second is as a right-handed one. Two threaded nuts (8 and 8′) are welded to the movable bars (6 and 6′) to move them through the rotation of the threaded rod. The rotation of this rod (7) is made via two wheels fixed at the two ends of the threaded rod. This rotation causes the movable bars to approach or to move away from each other according to the clockwise or anticlockwise direction of rotation, respectively.

At the two ends of the movable bars (6 and 6′), there are two small clamps (9 and 9′) used for fastening the two ends of the tested fiber (10) by an adhesive material. The fiber is put on a microscope slide (11), which is fixed and mounted on a metallic circular stage (12) 4.2 cm in diameter. Under the slide, there is a hole (1.8 cm in diameter) for the passage of light (13) punched into the principal base for light transmission.

The two movable bars (6 and 6′) move on a metric scale (14), on which the elongation or strain (ε) of the fiber can be measured. A spring balance (15) with an accuracy of ± 0.5 g is fixed from its two ends with movable bars. Upon the stretching of the fiber, the spring of the balance shows the actual mass needed to stretch the fiber, from which one can determine the corresponding stress (σ) or force on the fiber.

Part ii: Heating setup

The heating setup is shown in Figure 2 and consists mainly of three components.

Brass disk

This disk is designed with special dimensions (1.5 cm thick and 4 cm in diameter) to be fitted suitably to the fiber stage (12) shown in Figure 2. A hole (2 cm in diameter) for the passage of light is punched into the center of this disk to allow the incidence of light on the fiber and to the microscope objective, which can move up and down freely through this hole. This disk is provided with a special cavity (1 cm in diameter and 2.6 cm depth) to support the heater (hot finger) inside it. The heater (110 V and 3 A) has a cylindrical cross section 1 cm in diameter and 2.5 cm long. The bottom of the principal base (1) is perfectly lagged by a thermal isolator to minimize the heat loss and protect the microscope from heat during the heating process.

Temperature controller

The temperature of the tested fiber can be measured and controlled with a suitable control unit (temperature controller; 220 V and 50 Hz), which consists of a sensitive thermocouple and a digital recording element ranging from 0 to 200°C with a sensitivity of ± 0.5°C.

Alternating current (AC) varic

The rate of heating (0.5°C/min) of the fiber can be varied and controlled with an AC varic (220 V and 50 Hz) ranging from 0 to 270 V.

Part iii: Cooling setup

The cooling part is shown in Figure 3 and consists of the following.

Metallic base

This base is made from steel with suitable dimensions (13 cm long, 13 cm wide, and 0.15 cm thick) to be fitted with the fiber stage (12) shown in Figure 1. The base is coated from the bottom with a thermal isolating material. In the center of this base, there is a hole (0.2 cm in diameter) that allows the light to pass through it. A

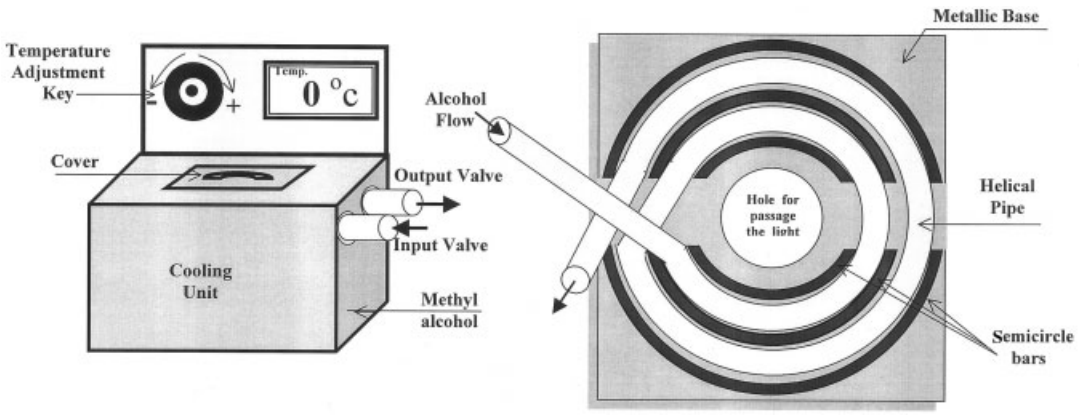

Figure 3 Schematic diagram of the cooling setup.

helical pipe (0.12 cm in diameter) made from copper is open-ended to allow methyl alcohol to enter from one end and emerge from the other. This pipe is enclosed between a group of semicircle bars fixed in the metallic base.

Cooling unit

This unit (220 V and 50 Hz) consists of a cubic container filled with methyl alcohol, which is transferred to the helical pipe via two (output and input) valves, and a fine temperature-adjustment key. With this key, the temperature of the alcohol can be reduced and controlled from room temperature (ca. 18°C) to 0°C.

The main purposes of the designed OTM device are

1. To study the variation of the optical properties (e.g., refractive indices, Δn, and polarizabilities) of fibers with the mechanical properties (σ–ε or drawing and stretching) with the drawing setup (part i) attached to the polarizing interference (Pluta) microscope.
2. To study the dependence of the optical properties of fibers on the temperature, from 0 to 50°C, with

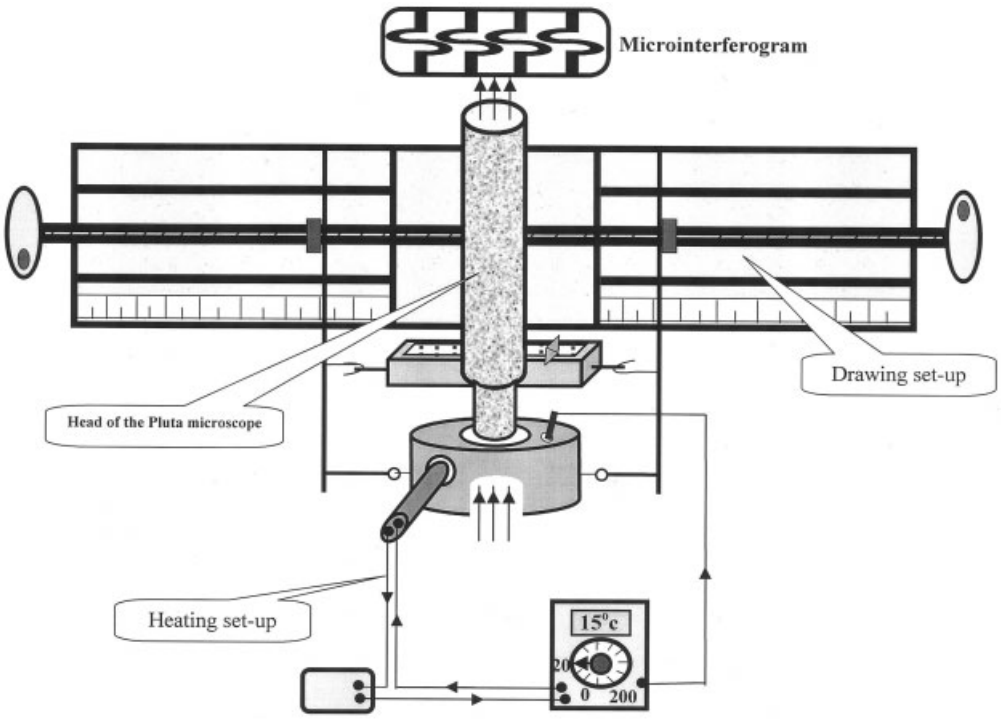

Figure 4 Schematic diagram of the combination parts i and ii of the OTM device attached to the Pluta polarizing interference microscope.

the heating setup (part ii) and cooling setup (part iii) attached to the Pluta microscope.
3. To study the correlation between both the mechanical and thermal properties of fibers with the optical properties.

OPERATING PROCEDURE FOR THE OTM DEVICE

Optothermal technique (with parts ii and iii of the OTM device)

The OTM device attached to the Pluta microscope can be used to study the influence of the temperature (0–50°C) on the optical properties of a sample from HDPE fibers. This study is performed in two sequences.

Cooling setup

1. With reference to Figures 1 and 3, the PE fiber is fixed by the two clamps (9 and 9′) and immersed in a suitable liquid on the microscope slide.
2. The metallic base of the cooling setup is fitted around the fiber stage of the OTM device. The helical pipe (Fig. 3) is connected to the valves of the cooling unit, which pushes the alcohol inside it.
3. Via the fine adjustment key of the cooling unit and the temperature controller, the temperature of the PE fiber is adjusted to 0°C. At this fixed temperature, the corresponding microinterferogram of a duplicated image of the fiber is photographed, and from this, $n^{\parallel}$ and $n^{\perp}$ of the PE fiber are determined.
4. Step 3 is repeated for different temperatures ranging from 0 to room temperature (18°C).

Heating setup

A heating process (from 18 to 50°C) for the same PE fiber is performed as follows:

1. The metallic base (Fig. 3) is replaced by the brass disk (Fig. 2), which is fitted on the fiber stage of the OTM device. Also, the cooling unit is replaced by the heater, which is inserted into the disk cavity and connected in series to the AC varic and the temperature controller.
2. Via the AC varic and the temperature controller, the temperature of the PE fiber is raised and controlled. At this temperature, the corresponding microinterferogram (duplicated image) of the fiber is photographed, and from this, the refractive indices of the PE fiber are determined.
3. Step 2 is repeated for different temperatures ranging from room temperature (18°C) to 50°C.

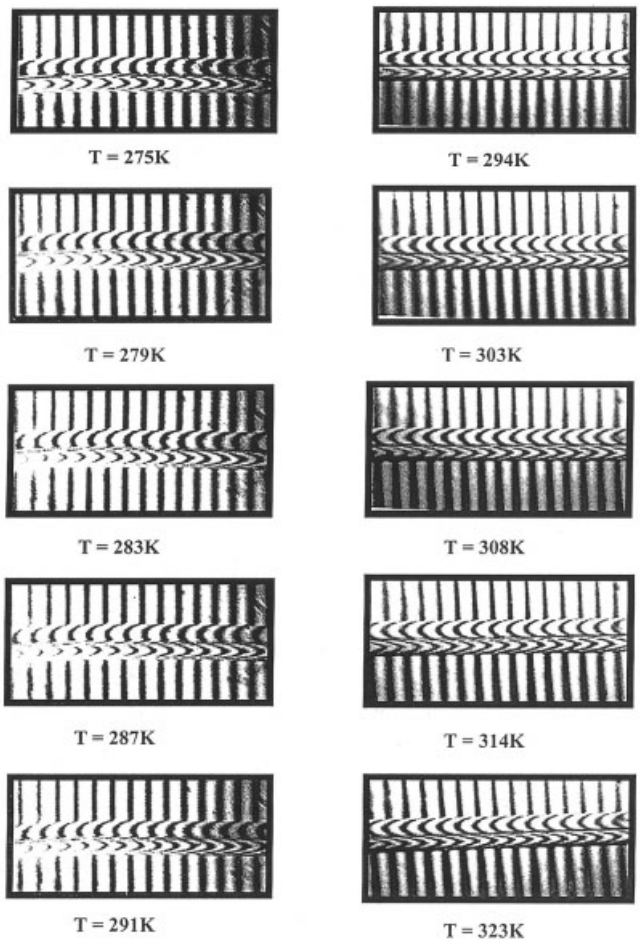

Figure 5 Microinterferograms of duplicated images for PE fibers at different temperatures (273–323 K) from the Pluta microscope.

The cooling and heating processes can be combined to study the effect of the temperature on the optical properties of PE fibers from 0 to 50°C. This range of temperature is used for environmental reasons, in that it covers the weather conditions of hot countries and serves the uses of PE fibers in many industries.

OTM technique (with parts i and ii of the OTM device)

The OTM device (parts i and ii) with the Pluta microscope (see Fig. 4) can be used to study the dependence of the optical properties of a sample from undrawn PP fibers on the mechanical properties (σ–ε or stretching/drawing) at different values of a fixed temperature ranging from 10 to 50°C in steps of 5°C as follows:

1. The PP fiber (8 cm long) is fixed with an adhesive material from the two ends of the two clamps (9 and 9′) shown in Figure 4 and is immersed in a suitable liquid on the microscope slide (11), which is fitted to the fiber stage (12).

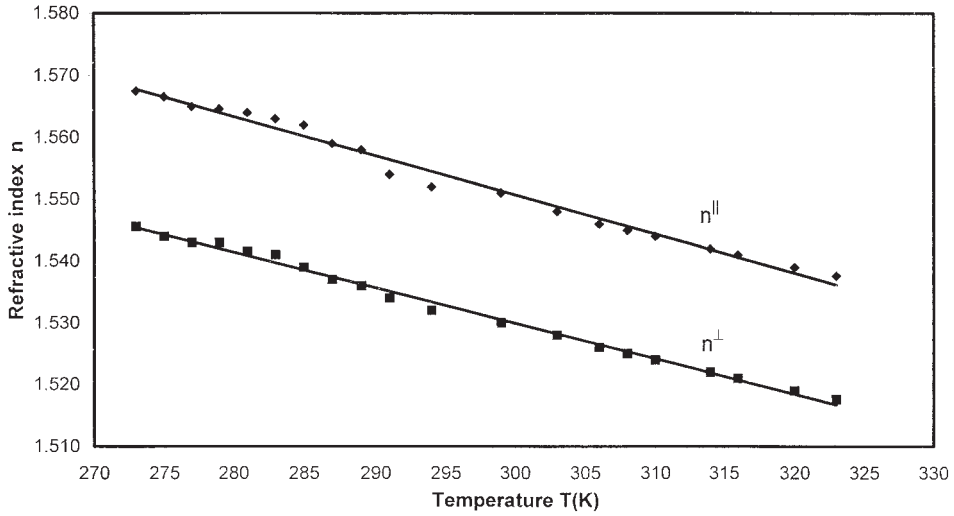

Figure 6 n of PE (D = 7.5) fibers versus the temperature.

2. At a fixed temperature with the heating setup, the PP fiber is stretched in steps of 4 cm as an elongation (0.5 D), and the reading of the spring balance (15), mass M, is recorded for each step of stretching. Then, the obtained microinterferogram of the duplicated image of the fiber is photographed at each value of stretching, from which the fiber diameter (t) and its cross-sectional area [$\pi(t/2)$] are determined. Hence, the applied stress on the fiber can be calculated.
3. The aforementioned steps (1 and 2) are repeated at different fixed temperatures greater than room temperature.

In step 2, the drawing conditions are as follows: (1) the stretching rate of the fiber is constant in all measurements [i.e., the number of revolutions per minute for threaded rod 7 (see Fig. 4) should be constant and equal to 6 rpm), and (2) the extension time (5 min/step) and the rate of heating (2°C/min) of the fiber are constant in all readings.

THEORETICAL CONSIDERATIONS

Molecular polarizability (P_M) of polymeric material

The polarization of a collection of atoms or molecules can arise in two ways. First, the applied field distorts the charge distributions and so produces an induced dipole moment in each molecule. Second, the applied field tends to line up the initially randomly oriented ξ_0 values of the molecules. p_i (electronic and ionic) was reported by Jackson:[16]

$$p_i = \frac{q^2}{m\omega_o^2} \tag{1}$$

where q is the molecule charge, m is the molecule mass, and ω_o is the oscillation frequency. ξ_0 is oriented and produces the orientation polarizability (p_o) as follows:

$$p_0 = \frac{1}{3K_BT}\xi_0^2 \tag{2}$$

where K_B is the Boltzmann constant and T is the temperature (K). In a general form, P_M is the summation of eqs. (1) and (2):

$$P_M = p_i + \frac{\xi_0^2}{3K_B}\frac{1}{T} \tag{3}$$

P_M is related to $n^{\parallel}$ and $n^{\perp}$ of the fiber in the following manner:[17]

$$P_M^j = \frac{3}{4\pi}\left(\frac{n_j^2 - 1}{n_j^2 + 2}\right) \tag{4}$$

Equation (3) gives the relation between ($1/T$) and P_M; with this relation, p_i can be determined from the intercept of the line with the P_M axis, and ξ_0 can be determined from the slope of the line. Where n_j is the refractive index of fiber and j denotes the state of light polarization ($\parallel$ or $\perp$).

σ–ε curves of undrawn fibers

One of the most common methods of strengthening the structure of a polymeric material is drawing it during processing. The strength of the polymer is its ability to withstand a load without breaking. This strength is characterized by σ, which causes failure.

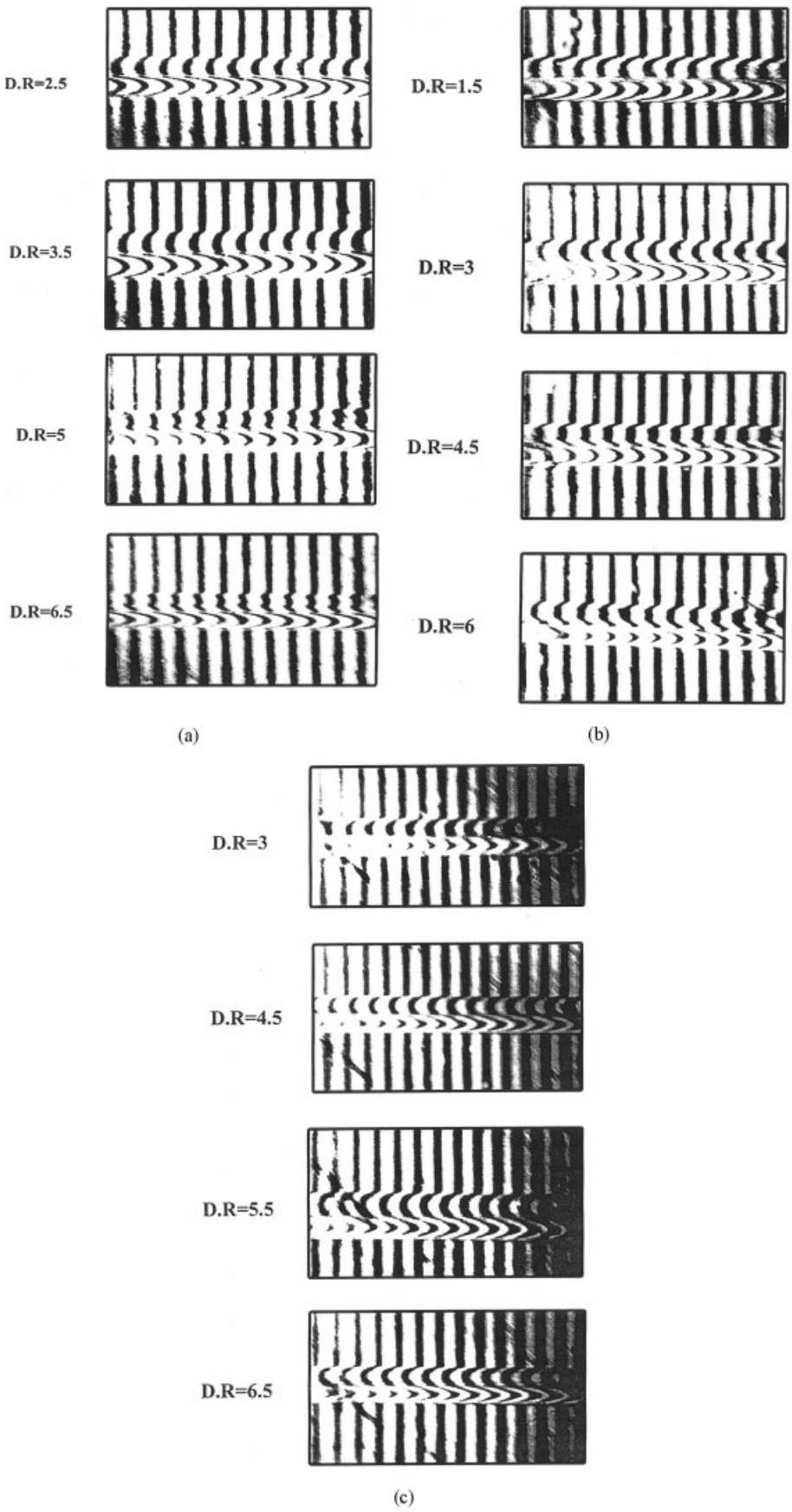

Figure 7 Set of microinterferograms representing the two-beam interference duplicated images of PP fibers with $\lambda = 546$ nm at different D values and temperatures of (a) 20, (b) 30, and (c) 40 °C.

This σ is called the tensile stress [ultimate strength (σ_s)], which is determined from the σ–ε curve. Also from this σ–ε curve, the elasticity of the fiber can be evaluated via σ_y and Young's modulus (E).[2] ε of fibers can be calculated as follows:[1]

$$\varepsilon = \ln D = \ln(L/L_0) \tag{5}$$

where L_0 and L are the lengths of the sample before and after deformation. Consequently, the resulting changes in cross section A of the fiber affect the actual σ value:

$$\sigma = F/A \tag{6}$$

where $F = Mg$ is the applied tensile force, M is the mass (load), and g is the acceleration due to gravity.

W' of fibers

W' for a collection of chains will depend on the distribution of chain-end distances and can be obtained with the following equation:[18]

$$W' = \frac{3K_BT}{2}\left[\frac{1}{3}(D^2 - D^{-1}) + (D^{-1} - 1)\right] \tag{7}$$

where T is the absolute temperature. This equation can be represented (W' vs D) at different T values.

RESULTS AND DISCUSSION

Optothermal behavior of PE fibers

The main purpose of this study (optothermal) is to use a cooling and heating setup (see Figs. 2 and 3) of an OTM device for the investigation of fiber properties. A suitable sample for this is HDPE fiber with $D = 7.5$. Monochromatic light with a wavelength of $\lambda = 546$ nm has been used. The refractive index of the immersion liquid (n_L) is 1.5205 at room temperature (293 K), and its optothermal coefficient is $dn_L/dT = -5 \times 10^{-4}$ K^{-1}.

The refractive index of any fiber is the main optical parameter from which most of the other optical and structural properties of the fiber can be optimized. Therefore, $n^{\parallel}$ and $n^{\perp}$ of the fiber are measured via the obtained microinterferograms and the following equation:[19]

$$n^j = n_L \pm \frac{Z^j\lambda}{ht} \tag{8}$$

where j denotes the state of light polarization ($\parallel$ or $\perp$), Z is the fringe shift displacement, and h is the interfringe spacing.

Figure 5 shows some of these microinterferograms of a duplicated image of PE fibers at different temperatures. Figure 6 illustrates the relationship between these refractive indices of the PE fibers and the temperature (273–323°K), showing inversely proportional behavior. The increase in the temperature reduces the values of the shift factor, which reflects the friction between the chain segments.[2] This decrease in the shift factor leads to an increase in the molecular mobility, reducing the density and hence reducing the refractive index of the fibers. From the obtained graphs, the optothermal coefficient of the PE ($D = 7.5$) fibers has been calculated ($dn/dT = -6 \times 10^{-4}$ K^{-1}).

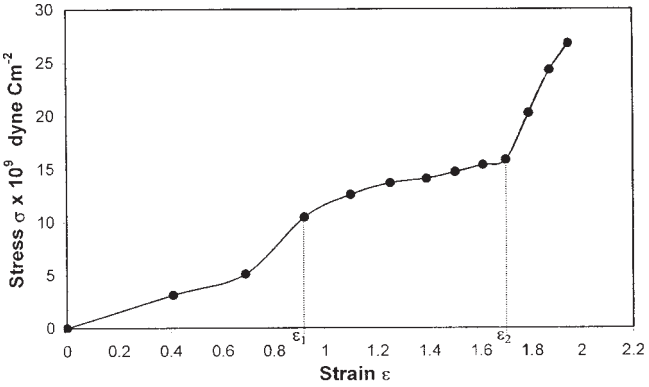

Figure 8 σ–ε curve of PP fibers at room temperature.

OTM behavior of PP fibers

The main purpose of this study (OTM) is to use a drawing-and-heating setup (see Figs. 1 and 2) of an OTM device for the investigation of fibers. A suitable sample for this is undrawn PP fibers. Also, the same value of λ (546 nm) has been used. n_L is 1.489 at room temperature (10°C). Some of the microinterferograms for these fibers (with different D values) for the light vibrating parallel and perpendicularly to the fiber axis are shown in Figure 7(a–c) at different temperatures (20, 30, and 40°C). The obtained experimental results for the PP fibers with the OTM device (Fig. 4) attached to the interference Pluta microscope are given and discussed in the following sections.

σ–ε curve of PP fibers

According to the experimental procedure of the OTM device and eqs. (5) and (6), the σ–ε curve of PP fibers can be obtained at room temperature (10°C), as shown in Figure 8. For a polymeric fiber, there is more than a shape of the σ–ε curve that characterizes the type of polymer. The obtained curve for PP fibers (Fig. 8) can be described by a sigmoidal (first convex and then concave) σ–ε curve.[1] In Figure 8, there are two distinguished elongation points ($\varepsilon_1 = 0.92$ and $\varepsilon_2 = 1.7$), which are the limits of the instability condition ($d\sigma/d\varepsilon \approx 0$). In the range of small elongations ($\varepsilon < \varepsilon_1$), the

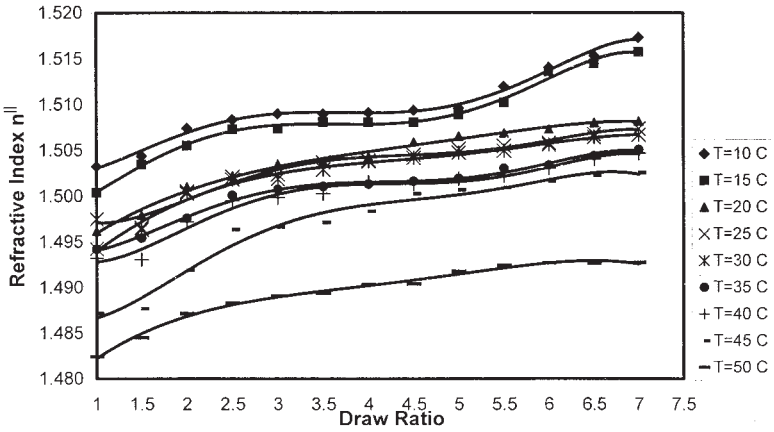

Figure 9 Relationship between $n^{\parallel}$ and D (1–7) of PP fibers at different temperatures.

deformation is uniform and is accompanied by a reduction of $E = d\sigma/d\varepsilon$. This deformation is usually reversible, and E is 7.1 × 10 dyn/cm in this range. In the intermediate range (plateau) of $\varepsilon_1 < \varepsilon < \varepsilon_2$, the deformation is irreversible. The critical σ value corresponding to point ε_1 is $\sigma_y = 10.46 \times 109$ dyn/cm^2. When the other critical point ε_2 is reached, further deformation is again reversible and uniform, followed by breakage of the sample. The σ value corresponding to this breakage is $\sigma_s = 26.78 \times 10$ dyn/cm. This behavior of σ–ε (Fig. 8) is most typical of polymeric fibers at temperatures not too high but higher than T_g.

$n^{\parallel}$ and $n^{\perp}$ of PP fibers

The refractive index is the major physical quantity that links the optical and structural (mechanical and thermal) properties of any fiber. Therefore, with eq. (8) and the captured microinterferograms, $n^{\parallel}$ and $n^{\perp}$ of PP fibers have been measured experimentally and are shown in Figures 9 and 10, respectively. In Figure 9, $n^{\parallel}$ is plotted against D (1–7) at different temperatures (10–50°C). $n^{\parallel}$ increases as D increases but decreases when the temperature increases. $n^{\perp}$ decreases as both the D value and temperature increase, as shown in Figure 10. The increase in D means a decrease in t and an increase in the molecular orientation of the chains. According to this fact and eq. (8), an increase in $n^{\parallel}$ and a decrease in $n^{\perp}$ occur, whereas the effect of the temperature on $n^{\parallel}$ and $n^{\perp}$ produces the same behavior mentioned previously for PE fibers.

According to the σ–ε curve (Fig. 8), points ε_1 and ε_2 are marked on the graph to limit the plateau (intermediate) region. In this region ($0.92 < \varepsilon < 1.7$), the deformation is irreversible (stable). This region can be defined by D instead of ε [see eq. (5)]. Therefore, this intermediate range of D values ($2.5 \leq D \leq 5.5$) is selected to avoid some problems from low drawing (the formation of clusters, networks, necking, and microcracks) and high drawing (recovery and cutting/breakage).[20–23] To correlate $n^{\parallel}$ of PP fibers with both D (within the intermediate range) and T, the relationship in Figure 9 has been fitted in this range and replotted. A straight-line relationship between $n^{\parallel}$ and D has been

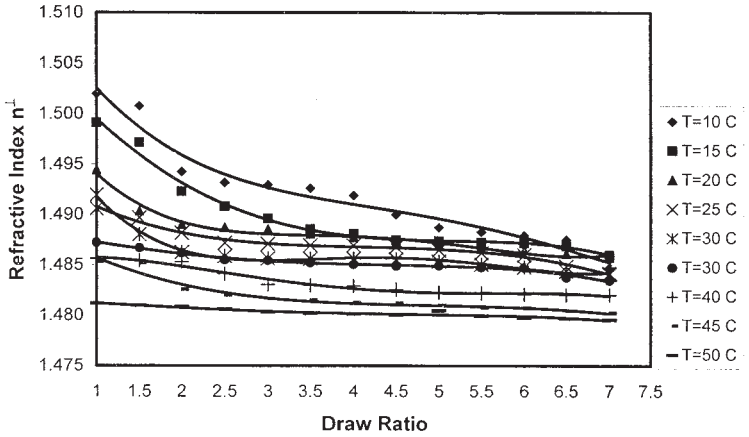

Figure 10 Relationship between $n^{\perp}$ and D (1–7) of PP fibers at different temperatures.

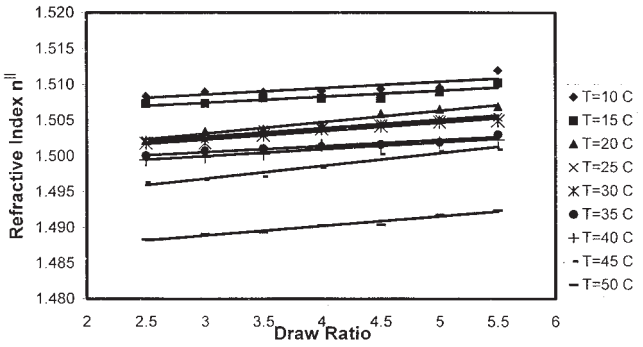

Figure 11 Relationship between $n^{\parallel}$ and D (2.5–5.5) of PP fibers at different temperatures.

obtained, as shown in Figure 11. Because of the important effects of T and D on the stretching process of polymer fibers, the following formula is suggested for PP fibers:

$$n^{\parallel}(D,T) = n_0 + \alpha(D-1) + \beta T^2 \qquad (9)$$

where n_0 is the isotropic refractive index at 0°C, α is the optodrawing coefficient, and β is the optothermal coefficient. The values of these constants for PP fibers are $n_0 = 1.508$, $\alpha = 0.001$, and $\beta = -7 \times 10^{-6}$ (°C)$^{-2}$. The accuracy of measuring the refractive index of PP fibers (fitting between this formula and the experimental data) is ± 0.001 at $2.5 \le D \le 5.5$ and $10°C \le T \le 50°C$).

Generally, to apply eq. (9) for any polymeric fiber, the constants n_0, α, and β should be determined as follows:

1. The refractive index ($n = n^{\parallel}$) should be measured at three different D values (D_1, D_2, and D_3) at a constant value of T. Substituting the values of the calculated refractive indices (n_1, n_2, and n_3) into eq. (9), we obtain the following equations:

$$n_1(D_1,T) = n_0 + \alpha(D_1 - 1) + \beta T^2 \qquad (10a)$$

$$n_2(D_2,T) = n_0 + \alpha(D_2 - 1) + \beta T^2 \qquad (10b)$$

$$n_3(D_3,T) = n_0 + \alpha(D_3 - 1) + \beta T^2 \qquad (10c)$$

2. With this set of equations solved, we can obtain the constants (n_0, α, and β) as follows:

$$n_0 = \frac{\Delta_1}{\Delta}$$

$$\alpha = \frac{\Delta_2}{\Delta}$$

$$\beta = \frac{\Delta_3}{\Delta}$$

where

$$\Delta = \begin{vmatrix} 1 & D_1 - 1 & T^2 \\ 1 & D_2 - 1 & T^2 \\ 1 & D_3 - 1 & T^2 \end{vmatrix} \qquad \Delta_1 = \begin{vmatrix} n_1 & D_1 - 1 & T^2 \\ n_2 & D_2 - 1 & T^2 \\ n_3 & D_3 - 1 & T^2 \end{vmatrix}$$

$$\Delta_2 = \begin{vmatrix} 1 & n_1 & T^2 \\ 1 & n_2 & T^2 \\ 1 & n_3 & T^2 \end{vmatrix} \qquad \Delta_3 = \begin{vmatrix} 1 & D_1 - 1 & n_1 \\ 1 & D_2 - 1 & n_2 \\ 1 & D_3 - 1 & n_3 \end{vmatrix}$$

3. Finally, with eq. (9), n of any polymeric fiber may be expected at any D ($2.5 \le D \le 5.5$) and any value of T ($10°C \le T \le 50°C$).

Molecular polarizabilities ($\boldsymbol{P}_M^{\parallel}$ and $\boldsymbol{P}_M^{\perp}$) of PP fibers

$P_M^{\parallel}$ and $P_M^{\perp}$ of PP fibers have been calculated via eq. (3) and plotted against the reciprocal of the temperature ($1/T$) at different D values in Figures 12 and 13. Each of these figures represents eq. (3), which helps us to evaluate two different types of polarization (p_i and ξ_0

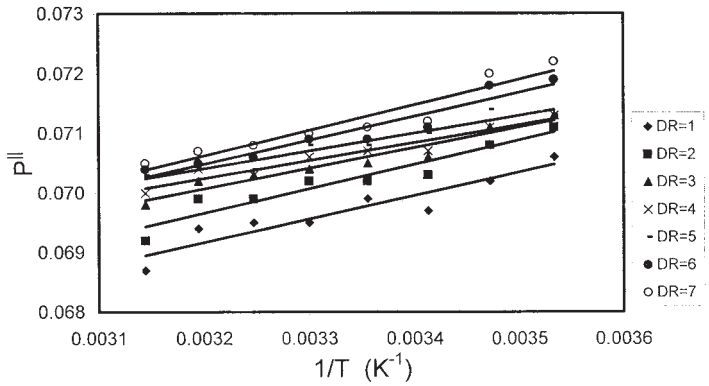

Figure 12 Relationship between $P^{\parallel}$ and T (10–45°C) of PP fibers at different D values.

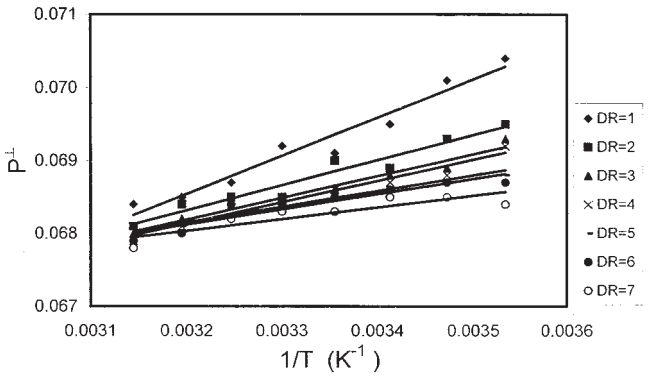

Figure 13 Relationship between $P^{\perp}$ and T (10–45°C) of PP fibers at different D values.

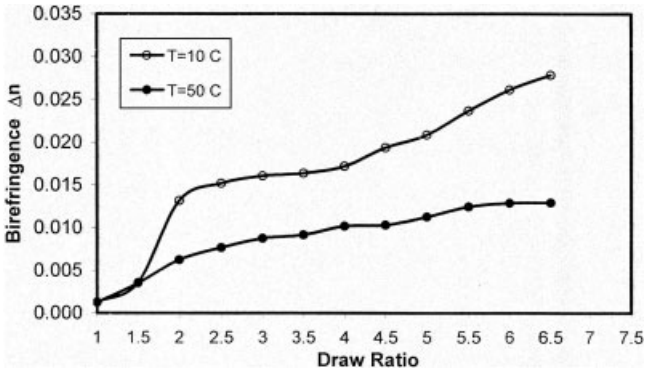

Figure 14 Relationship between Δn and D (1–7) of PP fibers at different temperatures.

for ∥ and ⊥ light vibrations) at different D values. The values obtained for the investigated PP fibers are presented in Table I.

Δn of PP fibers

Δn is an important physical parameter that links the optical and mechanical properties of fibers. Figure 14 shows the dependence of Δn ($\Delta n = n^{\parallel} - n^{\perp}$) on D for PP fibers at two different temperatures (10 and 50°C). In this figure, Δn increases as D increases for two possible reasons: the reduction of the amorphous orientation by the chain relaxation[3] and the net difference between the increase in $n^{\parallel}$ and the decrease in $n^{\perp}$ with the increase in D for PP fibers.

"The textile characteristics of man-made (isotropic) fibers can be improved by the mechanical drawing, which results in stronger, more birefringent fibers that are highly anisotropic."[2,4] In Figure 14, the drawing of PP fibers at 10°C produces higher values of Δn than drawing at 50°C. According to this result and Figure 14, the drawing of PP fibers at low temperatures (cold drawing) is recommended. It may be [more] useful than that at higher temperatures.

W' of PP fibers

With eq. (7), W' for PP fibers has been calculated and plotted versus D (1–7) at different temperatures (10–45°C) in Figure 15. The gradual increase in W' with D may be due to the increasing work done on the fibers and the increasing amount of associated deformation. Also, W' increases as the temperature rises; at low D values (<3), the influence of temperature is insignificant, but at high D values (>3), this effect is highly significant.

Figure 16 shows the relationship between W' and Δn for PP fibers at room temperature. In the intermediate range of the D values (2.5–5.5), this relationship is represented by a straight line, as shown in the following suggested formula:

$$\Delta n = k_1 W' + k_2$$

where constant k_1 is 2×10^{17} J^{-1} and constant k_2 is 0.016. Because of this empirical formula and eq. (7), it is clear that the increase in D leads to an increase in σ for the fiber, W', and Δn.

TABLE I
Induced Electronic and Ionic Polarizabilities ($p_i^{\parallel}$ and $p_i^{\perp}$) and Permanent Dipole Moments ($\zeta_0^{\parallel}$ and $\zeta_0^{\perp}$) of PP Fibers at Different D Values

D	$p_i^{\parallel}$	$p_i^{\perp}$	$\zeta_0^{\parallel}$ (10^{-11})	$\zeta_0^{\perp}$ (10^{-11})
1	0.057	0.052	1.27	1.47
2	0.057	0.057	1.30	1.19
3	0.060	0.059	1.19	1.11
4	0.061	0.059	1.11	1.10
5	0.061	0.061	1.11	0.94
6	0.058	0.062	1.29	0.93
7	0.057	0.063	1.33	0.82

CONCLUSIONS

An OTM device has been designed to study the correlation between the optical, thermal, and mechanical

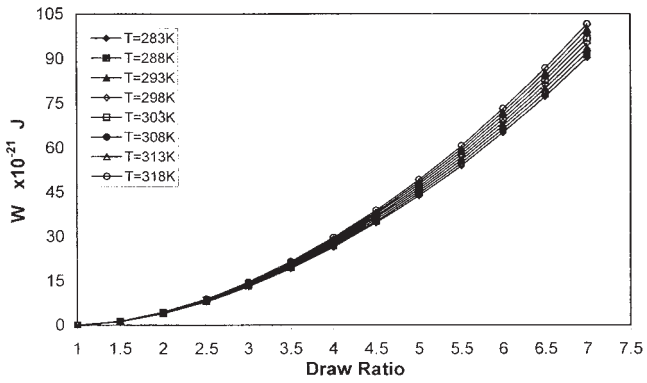

Figure 15 Relationship between W' and D (1–7) of PP fibers at different temperatures.

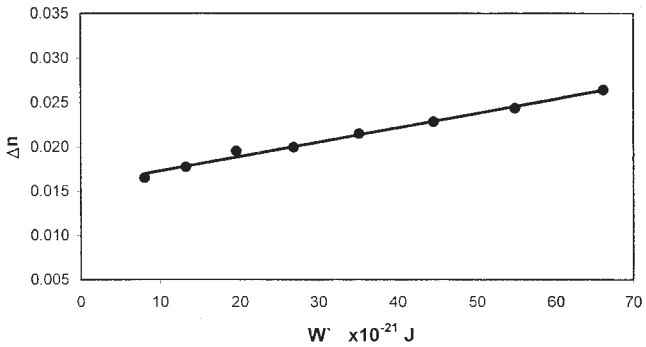

Figure 16 Relationship between W' and Δn of PP fibers at room temperature.

properties of fibers. The OTM device, connected to a Pluta microscope, provides an accurate and easy dynamical method for studying the OTM properties of the tested fibers and, therefore, for investigating any changes in the optical properties due to drawing, heating, or even both. As a result, the following points have been elucidated:

1. With the cooling and heating setup of the OTM device, the PE fiber has been investigated in an environmental temperature range (0–50°C). The refractive index of the PE fiber is inversely dependent on the temperature, and from this behavior, dn/dT has been determined.
2. With the drawing and heating setup of the OTM device, the OTM behavior for PP fibers has been evaluated.
3. The σ–ε curve of PP fibers can be described by a sigmoidal shape, which helps us to obtain important mechanical properties of fibers, such as σ_y, E, and σ_s.
4. A formula has been proposed to relate $n^{\parallel}$ of PP fibers to both D and T. This formula may enable us to predict the refractive index of polymeric fibers at different D values ($2.5 \leq D \leq 5.5$) and T values ($10°C \leq T \leq 50°C$).
5. Two different types of polarization (p_i and ξ_0) for PP fibers have been evaluated at different D values.
6. It is recommended that the drawing of PP fibers at low temperatures may be [more] useful than that at higher temperatures for obtaining more birefringent fibers.
7. The relationship between W' and D at different temperatures reflects the amount of deformation for PP fibers during the drawing and heating processes. Also, the relationship between W' and Δn has been studied and given in an empirical formula.

References

1. Walezak, Z. K. Formation of Synthetic Fibers; Gordon & Breach: New York, 1977.
2. Tager, A. Physical Chemistry of Polymers; Mir: Moscow, 1978.
3. Le Bourvellec, G.; Beautemps, J. J Appl Polym Sci 1990, 39, 329.
4. Gaur, A. H.; De Vries, H. J Polym Sci: Polymer Physics Edition 1975, 13, 835.
5. Hearle, J. W. S. J Appl Polym Sci 1963, 7, 1175.
6. Hearle, J. W. S. J Appl Polym Sci 1963, 7, 1193.
7. Pluta, M. Opt Acta 1971, 18, 661.
8. Pluta, M. J Microsc 1972, 96, 309.
9. Hamza, A. A.; Sokkar, T. Z. N.; El-Farahaty, K. A.; El-Dessouky, H. M. J Phys: Condens Matter 1999, 11, 5331.
10. Belal, A. E.; Hamza, A. A.; Sokkar, T. Z. N.; El-Farahaty, K. A.; Yassien, K. M. Polym Test 2002, 21, 877.
11. Hamza, A. A.; Fouda, I. M.; El-Farahaty, K. A.; Hellaly, S. A. J Polym Test 1987, 7, 329.
12. Hamza, A. A.; El-Farahaty, K. A.; Hellaly, S. A. Opt Appl 1988, 18, 133.
13. Hamza, A. A.; Sokkar, T. Z. N.; El-Bakary, M. A.; Ali, A. M. Polym Test 2003, 22, 83.
14. Tang, T.; Huang, B. J Appl Polym Sci 1994, 53, 355.
15. Colvin, R.; Moore, B. Mod Plast 1997, 74, 56.
16. Jackson, J. D. Classical Electrodynamics; John Wiley & Sons: New York, 1974; Chapter 4.
17. Lorentz, H. A. Ann Phys (NY) 1952, 9, 641.
18. Williams, D. J. Polymer Science and Engineering; Prentice-Hall: Englewood Cliffs, NJ, 1971.
19. Barakat, N.; Hamza, A. A. Interferometry of Fibrous Materials; Adam Hilger: Bristol, England, 1990.
20. Sova, M.; Raab, M.; Sližov, M. J Mater Sci 1993, 28, 6516.
21. Carothers, W. H.; Hill, J. W. J Am Chem Soc 1932, 54, 579.
22. Kilian, H. G.; Pietralla, M. Polymer 1978, 19, 664.
23. Purvis, J.; Bower, D. I. J Polym Sci: Polymer Physics Edition 1976, 14, 1461.